Rapid Communications

Search for stabilizing effects of the $Z = 82$ shell closure against fission

J. Gehlot,[1] S. Nath,[1,*] Tathagata Banerjee,[1,†] Ish Mukul,[1,‡] R. Dubey,[1,§] A. Shamlath,[2] P. V. Laveen,[2] M. Shareef,[2] Md. Moin Shaikh,[1,∥] A. Jhingan,[1] N. Madhavan,[1] Tapan Rajbongshi,[3,¶] P. Jisha,[4] and Santanu Pal[1,#]

[1]*Nuclear Physics Group, Inter-University Accelerator Centre, Aruna Asaf Ali Marg, Post Box 10502, New Delhi 110067, India*
[2]*Department of Physics, School of Mathematical and Physical Sciences, Central University of Kerala, Kasaragod 671314, India*
[3]*Department of Physics, Gauhati University, Guwahati 781014, India*
[4]*Department of Physics, University of Calicut, Calicut 673635, India*

(Received 15 March 2019; revised manuscript received 20 May 2019; published 27 June 2019)

Background: Presence of closed proton and/or neutron shells causes deviation from macroscopic properties of nuclei, which are understood in terms of the liquid-drop model. Efforts to synthesize artificial elements are driven by the prediction of the existence of closed shells beyond the heaviest doubly magic nucleus found in nature. It is important to investigate experimentally the stabilizing effects of shell closure, if any, against fission.
Purpose: This Rapid Communication aims to investigate probable effects of proton shell ($Z = 82$) closure in the compound nucleus in enhancing survival probability of the evaporation residues formed in heavy ion-induced fusion-fission reactions.
Method: Evaporation residue cross sections have been measured for the reactions $^{19}F + ^{180}Hf$, $^{19}F + ^{181}Ta$, and $^{19}F + ^{182}W$ from $\simeq$9% below to $\simeq$42% above the Coulomb barrier; leading to the formation of compound nuclei with the same number of neutrons ($N = 118$) but different numbers of protons across $Z = 82$ employing the Heavy Ion Reaction Analyzer. Measured excitation functions have been compared with a statistical model calculation in which the reduced dissipation coefficient is the only adjustable parameter.
Results: Evaporation residue cross section, normalized by the capture cross section, is found to decrease gradually with increasing fissility of the compound nucleus. Measured evaporation residue cross sections require inclusion of nuclear viscosity in the model calculations. Reduced dissipation coefficient in the range of 1–3 $\times$ 10^{21} s^{-1} reproduces the data quite well.
Conclusions: Since entrance channel properties of the reactions and structural properties of the heavier reaction partners are very similar, the degree of presence of noncompound nuclear fission, if any, is not expected to be significantly different in the three cases. No abrupt enhancement of evaporation residue cross sections has been observed in the reaction forming a compound nucleus with $Z = 82$. Thus, this Rapid Communication does not find enhanced stabilizing effects of the $Z = 82$ shell closure against fission in the compound nucleus. One may attempt to measure cross sections of individual exit channels for further confirmation of our observation.

DOI: 10.1103/PhysRevC.99.061601

I. Introduction. Bohr and Wheeler [1] modeled the atomic nucleus as a homogeneously charged liquid drop. Many macroscopic properties of nuclei, most notably the phenomenon of fission [2] in which a heavy nucleus splits itself into lighter fragments, could be understood in terms of the liquid-drop model (LDM). However, limitations of this model to explain microscopic features, e.g., enhanced stability of a few nuclei, led to the development of the nuclear shell model by Mayer and others [3]. Since then, effects of shells on nuclear reaction dynamics has been a topic of great interest. Most significantly, superheavy nuclei, beyond the heaviest nucleus available in nature, have been hypothesized to exist solely because of shell stabilization effects. Sustained efforts in the field of heavy element research since the first prediction [4] of a doubly shell-closed nucleus beyond $^{208}_{82}Pb_{126}$, culminated recently into completion of the seventh period of the periodic table of elements [5]. Although the trans-lead doubly shell-closed nucleus is yet to be synthesized in a laboratory, the cardinal role of shell stabilization in enhancing the lifetime of superheavy nuclei has been firmly established [6].

Formation cross sections of superheavy evaporation residues (ERs) being vanishingly small, it is rather

*subir@iuac.res.in
†Presently at the Department of Nuclear Physics, Research School of Physics and Engineering, The Australian National University, Canberra ACT 2601, Australia.
‡Presently at TRIUMF, 4004 Wesbrook Mall, Vancouver, British Columbia V6T 2A3, Canada.
§Presently at iThemba LABS, National Research Foundation, P.O. Box 722, 7129 Somerset West, South Africa.
∥Presently at the Physics Group, Variable Energy Cyclotron Centre, 1/AF Bidhan Nagar, Kolkata 700064, India.
¶Presently at Central Research Hub, Assam Science and Technology University, Guwahati 781013, India.
#Formerly with the Physics Group, Variable Energy Cyclotron Centre, 1/AF Bidhan Nagar, Kolkata 700064, India.

TABLE I. Details of the nuclear reactions studied in this Rapid Communication. β_2, V_B, Q_{CN}, χ_{CN}, and η_{BG} are the quadrupole deformation, the Coulomb barrier, Q value of the reaction, CN fissility, and the Businaro-Gallone critical mass asymmetry, respectively. Z_pZ_t and $\eta = \frac{|A_p-A_t|}{(A_p+A_t)}$ are entrance channel charge product and mass asymmetry, respectively. Here Z_p (Z_t) and $A_p(A_t)$ respectively denote atomic number and mass number of projectile (target).

System	β_2 (target)	V_B (MeV)	Z_pZ_t	η	CN	Q_{CN} (MeV)	χ_{CN}	η_{BG}
${}^{19}_{9}F_{10} + {}^{180}_{72}Hf_{108}$	0.274	76.8	648	0.809	${}^{199}_{81}Tl_{118}$	−23.210	0.691	0.831
${}^{19}_{9}F_{10} + {}^{181}_{73}Ta_{108}$	0.269	77.9	657	0.810	${}^{200}_{82}Pb_{118}$	−23.678	0.701	0.838
${}^{19}_{9}F_{10} + {}^{182}_{74}W_{108}$	0.259	79.0	666	0.811	${}^{201}_{83}Bi_{118}$	−28.314	0.712	0.844

challenging to study the dynamics of such reactions. Several studies on effects of shell closure on reaction dynamics, therefore, have been reported in the mass region around ${}^{208}_{82}Pb_{126}$. One important difference between the nuclei in the vicinity of $Z = 82$, $N = 126$ and the superheavy nuclei, although, should be borne in mind. Whereas the fission barrier in the latter arises solely because of shell effects, the liquid-drop model accounts for a substantive part of the fission barrier in the former. The first comprehensive investigation to verify reduction of fission competition in deexcitation of the compound nucleus (CN) due to stabilizing influence of the strong ground-state shell effect in the vicinity of $N = 126$ was reported by Vermeulen *et al.* [7]. However, the results showed "surprisingly" low stabilizing influence of the spherical shell against fission competition. Andreyev *et al.* [8] studied systematics of ER cross sections (σ_{ER}) for the neutron-deficient compound nuclei ${}^{184-192}_{83}Bi^*$ and ${}^{186-192}_{84}Po^*$ formed in complete fusion between two heavy ions. A satisfactory reproduction of the data by the statistical model (SM) demanded up to 35% reduction of the fission barrier. Based on the systematic analysis, the authors concluded "strongly" increased fissility above the shell closure at $Z = 82$. Nath *et al.* measured σ_{ER} [9] and ER-gated CN angular momentum (ℓ) distribution [10] for ${}^{19}F + {}^{184}W$ and compared the results with those from neighboring systems. The fission barrier for the CN with $Z = 82$ was found to deviate from the systematic (N, Z) dependence. Similar measurements were carried out for the reactions ${}^{30}Si + {}^{170}Er$ and ${}^{31}P + {}^{170}Er$ forming the compound nuclei ${}^{200}_{82}Pb^*_{118}$ and ${}^{201}_{83}Bi^*_{118}$, respectively, by Mohanto and co-workers [11,12]. The results revealed no clear signature of extra stability due to $Z = 82$ shell closure, showing similar σ_{ER} and moments of the ℓ distribution for both reactions at a given $E_{c.m.} - V_B$. Here $E_{c.m.}$ stands for energy available in the centre of mass (c.m.) frame of reference.

These works relied upon SM of decay of the CN to interpret the data. This approach is questionable, in some cases, as reactions induced by heavier projectiles (e.g., ${}^{40}Ar$ [7] and ${}^{46}Ti$, ${}^{50,52}Cr$, and ${}^{94,95,98}Mo$ [8]) have been known to go through nonequilibrium processes, such as quasifission thereby inhibiting formation of the CN, equilibrated in all degrees of freedom. There are many recent studies in support of this argument [13,14]. The SMs used by various groups of researchers also differ in details. To explain the absence of "expected" stabilization against fission for spherical nuclei near $N = 126$, Junghans *et al.* [15] included collective enhancement of level density (CELD) in the calculation. *Ad hoc* reduction of the fission barrier was also suggested to reproduce measured σ_{ER} [8,12].

In this Rapid Communication, we revisit the question whether the $Z = 82$ shell closure enhances survival of ERs against fission. To improve upon earlier attempts, we have chosen three reactions to form compound nuclei with the same number of neutrons ($N = 118$) and different numbers for protons across $Z = 82$ (see Table I). The facts—(a) the reactions are induced by ${}^{19}F$ projectiles and (b) entrance channel parameters of the three reactions are nearly the same—lower the possibility of non-CN fission (NCNF) affecting ER formation significantly and with varying degree of severity in the three reactions. It is well known that shell effects tend to disappear at higher excitation energy (E^*). Recent measurements of fission fragment (FF) mass distribution from heavy compound nuclei [16,17] points to a *threshold* of $E^* \approx 40$ MeV up to which shell effects persist. The three compound nuclei are formed with E^* in the range of 42–92 MeV in the present experiment. The SM calculations performed in this Rapid Communication include all important physical phenomena known to affect fission dynamics and have a single adjustable parameter, viz. reduced dissipation coefficient β. Thus, scrutiny of results of the three reactions is expected to bring forth stabilizing influences of the $Z = 82$ shell closure against fission, if any.

II. The experiment. The experiment has been carried out at the 15UD Pelletron accelerator facility of the Inter-University Accelerator Centre (IUAC). A pulsed ${}^{19}F$ beam with pulse separation of 4 μs has been incident upon ${}^{180}Hf$ (150 $\mu g/cm^2$), ${}^{181}Ta$ (175 $\mu g/cm^2$), and ${}^{182}W$ (70 $\mu g/cm^2$) targets, all with thin (~20 $\mu g/cm^2$) ${}^{nat}C$ backing [18]. σ_{ER} have been measured employing the recoil mass spectrometer Heavy Ion Reaction Analyzer (HIRA) [19] at projectile energies (E_{lab}) in the range of 80–124 MeV. Two silicon detectos, placed inside the target chamber at $\theta_{lab} = 15.5^\circ$, have been used for absolute normalization of σ_{ER}. A thin (~30 $\mu g/cm^2$) ${}^{nat}C$ foil has been placed at $\theta_{lab} = 0^\circ$, 10.0 cm downstream from the target to ensure equilibrium charge state distribution of the ERs. ERs have been separated from the background events by the HIRA and transported to its focal plane to be detected by a multiwire proportional counter (MWPC). Time of flight (TOF) of the ERs has also been recorded. Further details about the experimental setup can be found elsewhere [20].

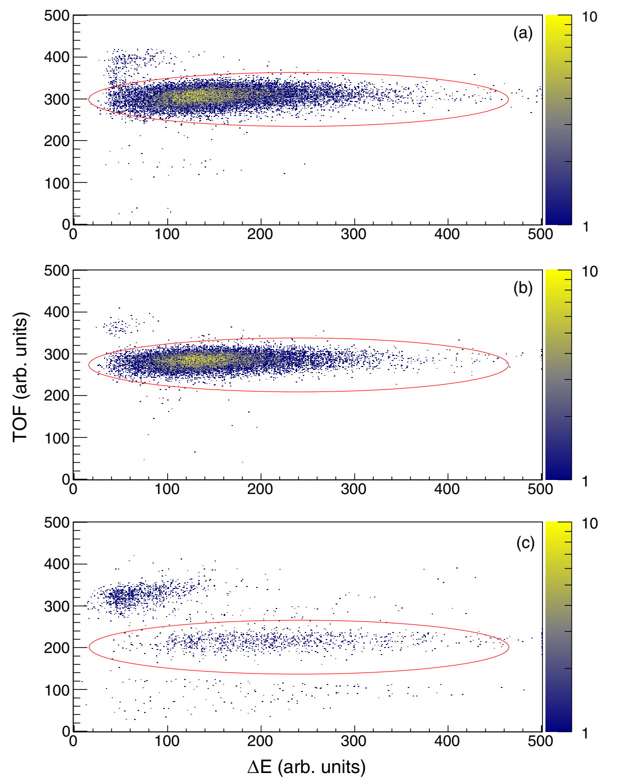

FIG. 1. Scatter plots between ΔE and TOF of the events recorded at the focal plane of the HIRA for (a) $^{19}F + {}^{180}Hf$ at $E_{lab} = 119.7$ MeV ($\frac{E_{c.m.}}{V_B} \simeq 1.41$), (b) $^{19}F + {}^{181}Ta$ at $E_{lab} = 99.6$ MeV ($\frac{E_{c.m.}}{V_B} \simeq 1.16$) and (c) $^{19}F + {}^{182}W$ at $E_{lab} = 79.6$ MeV ($\frac{E_{c.m.}}{V_B} \simeq 0.91$). ER events are enclosed within an elliptical gate in each plot.

III. Data analysis and results. The first step towards experimental determination of σ_{ER} is to identify the ERs unambiguously at the focal plane of the spectrometer. This is achieved by generating scatter plots between energy loss of ERs (ΔE) in the MWPC and their TOF. Three such plots for the three reactions are shown in Fig. 1. Inherent background rejection capability of the HIRA for very asymmetric reactions, such as the present ones, ensures that the ERs can be clearly separated from the few projectilelike particles reaching the focal plane. It is generally observed that the intensity of background events on the focal plane detector of the HIRA, although insignificant in most cases, increases gradually with decreasing E_{lab}. However, quite satisfactory separation between ERs and background events has been obtained over the entire range of E_{lab} in the present experiment.

The second most important aspect in the analysis is to estimate efficiency of HIRA (ϵ_{HIRA}). Only a fraction of ERs, produced in a fusion reaction, reaches the focal plane and is recorded by the detector. ϵ_{HIRA} for the ERs varies depending upon several reaction parameters. The same has been calculated employing the semimicroscopic Monte Carlo code TERS [21] following the formalism outlined in Ref. [9].

Measured σ_{ER} for the three reactions are shown in Fig. 2. The ER excitation function for $^{19}F + {}^{181}Ta$ had been reported earlier [22]. Nevertheless, we have measured σ_{ER} for this reaction along with the same for the other two reactions to ensure similar systematic errors, if any, in measured data. Our results for $^{19}F + {}^{181}Ta$ are in agreement with the same reported in Ref. [22] within experimental uncertainties.

IV. Statistical model calculation. The fate of a CN is decided in the present SM by following its time evolution through Monte Carlo sampling of the decay widths of various channels. Emission of neutrons, protons, α particles, and γ rays along with fission are considered as the probable channels of decay. A CN can undergo either fission with or without preceding evaporated particles and photons or reduce to an

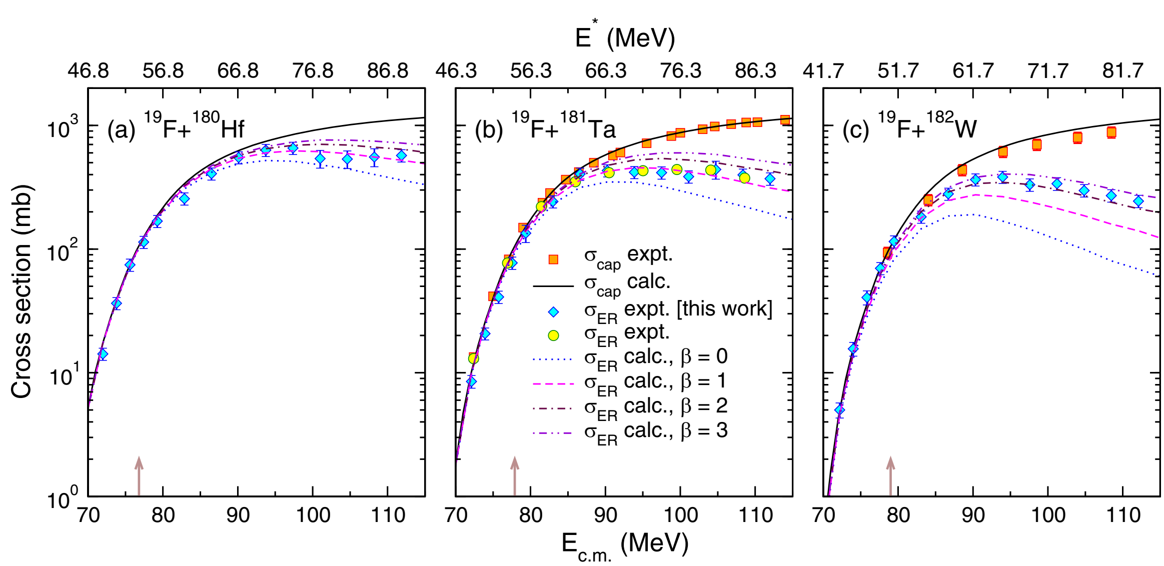

FIG. 2. Experimental and calculated σ_{ER} for (a) $^{19}F + {}^{180}Hf$, (b) $^{19}F + {}^{181}Ta$, and (c) $^{19}F + {}^{182}W$. Theoretical capture cross sections, calculated by CCFULL, are also shown for each system. Data points represented by filled (yellow) circles are obtained from Ref. [22]. The vertical arrow in each panel indicates the respective V_B.

ER. The final values of various observables are obtained as averages over a large ensemble of events. The fission width is obtained from the transition-state model of fission due to Bohr and Wheeler [1] with certain modifications as outlined below. The particle and γ-decay widths are obtained from the Weisskopf formula as given in Ref. [23].

We obtain the fission barrier in the present calculation by including a shell correction in the liquid-drop nuclear mass. Since the shell correction term δ is defined as the difference between the experimental and the LDM masses ($\delta = M_{\rm exp} - M_{\rm LDM}$), the full fission barrier $B_{\rm f}(\ell)$ of a nucleus carrying angular momentum ℓ is given as

$$B_{\rm f}(\ell) = B_{\rm f}^{\rm LDM}(\ell) - (\delta_{\rm g} - \delta_{\rm s}), \tag{1}$$

where $B_{\rm f}^{\rm LDM}(\ell)$ is the finite-range LDM fission barrier [24] and $\delta_{\rm g}$ and $\delta_{\rm s}$ are the shell correction energies at the ground state and the saddle configurations, respectively. The shell corrections at the ground state and the saddle are obtained following the recipe given in Ref. [25] for including deformation dependence in shell correction energy.

It is usually assumed that the orientation of the CN angular momentum remains perpendicular to both the reaction plane and the symmetry axis throughout the course of the reaction and the LDM fission barrier thus is obtained for $K = 0$, where K is the angular momentum component along the symmetry axis. However, the initial CN angular momentum direction can change its orientation due to perturbation by intrinsic nuclear motion [26]. Therefore, fission barriers for $K \neq 0$, which are larger than the $K = 0$ barrier, are also to be considered. This results in a reduction of the fission width which we have taken into account following Ref. [27].

The influence of the shell structure in nuclear single-particle levels in the nuclear level density which is used to calculate various decay widths of the CN is obtained from the works of Ignatyuk *et al.* [28] where the following form of the level-density parameter a is given

$$a(E^*) = \tilde{a}\left[1 + \frac{g(E^*)}{E^*}\delta\right], \tag{2}$$

where

$$g(E^*) = 1 - \exp\left(-\frac{E^*}{E_{\rm D}}\right), \tag{3}$$

and $E_{\rm D}$ is a parameter which determines the rate at which the shell effect decreases with an increase in E^*. The level-density parameter is shape dependent, and its asymptotic form $\tilde{a}$ at high E^* is taken from Ref. [29].

We next consider the CELD which arises due to the residual interaction giving rise to correlation among particle-hole states resulting in collective excitations. The total level-density $\rho(E^*)$ then can be written as [30]

$$\rho(E^*) = K_{\rm coll}(E^*)\rho_{\rm intr}(E^*), \tag{4}$$

where $\rho_{\rm intr}(E^*)$ is the intrinsic level density and $K_{\rm coll}$ is the collective enhancement factor.

The rotational ($K_{\rm rot}$) and vibrational ($K_{\rm vib}$) enhancement factors are taken from the work of Ignatyuk *et al.* [31]. A smooth transition from $K_{\rm vib}$ to $K_{\rm rot}$ with increasing quadrupole deformation $|\beta_2|$ of the CN is obtained using a function $\varphi(|\beta_2|)$ given as follows [32]:

$$K_{\rm coll}(E^*) = \{K_{\rm rot}\varphi(|\beta_2|) + K_{\rm vib}[1 - \varphi(|\beta_2|)]\}f(E^*), \tag{5a}$$

where

$$\varphi(|\beta_2|) = \left[1 + \exp\left(\frac{\beta_2^0 - |\beta_2|}{\Delta\beta_2}\right)\right]^{-1}. \tag{5b}$$

The values of $\beta_2^0 = 0.15$ and $\Delta\beta_2 = 0.04$ are taken from Ref. [33]. The following form of the function $f(E^*)$ accounts for the damping of collective effects with increasing excitation [15]:

$$f(E^*) = \left[1 + \exp\left(\frac{E^* - E_{\rm cr}}{\Delta E}\right)\right]^{-1}. \tag{6}$$

The values of $E_{\rm cr}$ and ΔE are taken as 40 and 10 MeV, respectively, which were obtained by fitting yields from projectile fragmentation experiments [15]. The lowest value of $K_{\rm coll}(E^*)$ is pegged at 1.

It is observed in numerous studies that a fission hindrance with respect to the Bohr-Wheeler fission width ($\Gamma_{\rm f}^{\rm BW}$) is required in order to reproduce prescission neutron multiplicity data from fusion-fission reactions (see, e.g., Ref. [26]). A reduction in fission width is obtained from the dissipative stochastic dynamical model of fission due to Kramers where the fission width is given as [34]

$$\Gamma_{\rm f}^{\rm Kram}(E^*, \ell, K) = \Gamma_{\rm f}^{\rm BW}(E^*, \ell, K)\left\{\sqrt{1 + \left(\frac{\beta}{2\omega_{\rm s}}\right)^2} - \frac{\beta}{2\omega_{\rm s}}\right\}, \tag{7}$$

where β is the reduced dissipation coefficient (ratio of the dissipation coefficient to inertia) and $\omega_{\rm s}$ is the frequency of a harmonic-oscillator potential which approximates nuclear potential in the saddle region. In a stochastic dynamical model of fission, the fission rate reaches its stationary value as given by Eq. (7) after elapse of a certain time interval [35]. We, therefore, use a parametrized form of time-dependent fission width as given in Ref. [36].

The above features are incorporated in a SM code VECSTAT [37]. Detailed application of the model is discussed elsewhere [38].

Decay widths and fission barrier depend upon the angular momentum of the CN. The ℓ distribution for capture are fed into the SM as input. Total and partial capture cross sections ($\sigma_{\rm cap}$ and σ_ℓ, respectively) at a given energy of the projectile can be calculated by the coupled-channels (CC) formalism. To this end, $\sigma_{\rm cap}$ for ^{19}F + ^{181}Ta [39] and ^{19}F + ^{182}W have been reproduced by the CC code CCFULL [40] incorporating appropriate potential parameters and couplings. $\sigma_{\rm cap}$ data for the latter reaction have been obtained by adding $\sigma_{\rm ER}$ (this Rapid Communication) and $\sigma_{\rm fiss}$ [41]. $\sigma_{\rm cap}$ and σ_ℓ for ^{19}F + ^{180}Hf have been calculated assuming potential parameters and a coupling scheme similar to the other two reactions.

In the present Rapid Communication, SM calculations are performed treating β as the only adjustable parameter. Results from the SM calculation with different values of β along with results of CC calculation are shown in Fig. 2.

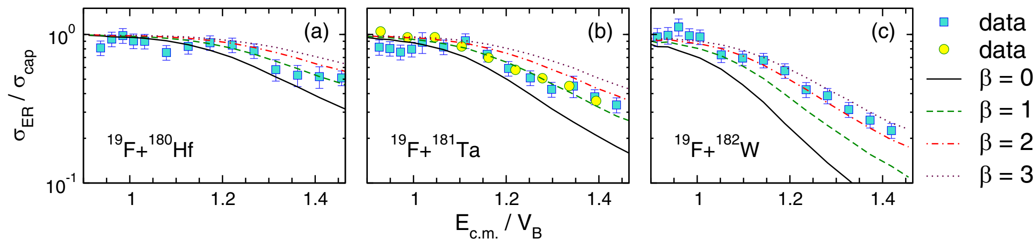

FIG. 3. Measured and calculated $\sigma_{\rm ER}$ normalized by theoretical $\sigma_{\rm cap}$ for (a) ^{19}F + ^{180}Hf, (b) ^{19}F + ^{181}Ta, and (c) ^{19}F + ^{182}W. Data points represented by filled (yellow) circles are obtained from Ref. [22].

V. Discussion. Effects of shell closure on nuclear reaction dynamics have been investigated through various observables. Enhanced FF anisotropy with respect to the prediction by the standard statistical saddle-point model, observed in ^{12}C + ^{198}Pt [42], was attributed to the effects of the $N = 126$ shell in the potential-energy surface (PES) of the CN. On the other hand, no signature of the modification of the PES due to the effect of the $N = 126$ shell closure was manifest in FF mass distribution [43] as the normalized width of mass distributions from ^{12}C + ^{194,198}Pt (leading to the CN with $N = 120$ and 126, respectively) was found to be almost identical. Influence of shell closure in the reaction partners on the mass and angle distributions of FFs [44]) and signatures of the $Z = 82$ shell closure in the α-decay process in heavy nuclei [45] have been reported in recent years.

Unlike FFs and neutrons, which may originate from both equilibrated compound nuclei and nonequilibrium processes, ERs are the most unambiguous signatures of CN formation. However, the theoretical reproduction of $\sigma_{\rm ER}$ is not always free from uncertainties. For heavy fissile systems, $\sigma_{\rm ER}$ can be expressed as

$$\sigma_{\rm ER}(E_{\rm c.m.}) = \sum_{\ell=0}^{\infty} \sigma_{\rm cap}(E_{\rm c.m.}, \ell) P_{\rm CN}(E_{\rm c.m.}, \ell) P_{\rm sur}(E^*, \ell), \quad (8)$$

where the three terms on the right-hand side of Eq. (8) denote: (a) the probability of the collision partners to overcome the potential barrier in the entrance channel, (b) the probability that the composite system will evolve into an equilibrated mononucleus starting from the touching configuration inside the fission saddle point, and (c) the probability that the CN will survive as a cold ER, respectively.

The second term on the right-hand side of Eq. (8), is the least precisely known. Considerable variance is also known to exist among the different SMs, which are frequently used to calculate the third term on the right-hand side of Eq. (8). Given these difficulties, comparing the ER excitation functions of three similar reactions and looking for signatures of the $Z = 82$ shell closure are quite challenging.

While trying to reproduce $\sigma_{\rm ER}$ with the SM for the decay of the CN, it is implicitly assumed that $P_{\rm CN} = 1$. In other words, the target-projectile composite system is assumed to yield an equilibrated CN and not to proceed towards nonequilibrium fissionlike processes. This assumption is questionable. Several studies on the presence of nonequilibrium processes in the 200-amu mass region have been reported. Shidling *et al.* interpreted reduction of $\sigma_{\rm ER}$ in ^{19}F + ^{181}Ta, compared to the same in ^{16}O + ^{184}W as a consequence of preequilibrium fission [46]. Nasirov *et al.* [39] performed a detailed analysis of these two reactions within the framework of the dinuclear system (DNS) model. According to the results from the DNS model, quasifission and fast fission cause hindrance to complete fusion in both reactions, albeit with varying degrees of severity. On the other hand, the study of FF mass distribution did not find any signature of quasifission for the reactions ^{19}F + ^{181}Ta and ^{16}O + ^{184}W [47].

In light of these conflicting reports, we argue that: (a) the presence of NCNF in the three ^{19}F-induced reactions under consideration is not significant, and (b) the influences of NCNF, if any, on $\sigma_{\rm ER}$ in these reactions are comparable as the entrance channel parameters $Z_{\rm p}Z_{\rm t}$, η and structural features of the targets are rather similar.

In reproducing observables from fusion-fission reactions, the input parameters in the SM, such as level density, fission barrier, and fission delay time are often varied in an *ad hoc* manner. In the present Rapid Communication, no parameter of the SM except for β is varied to interpret the data. Figure 2 shows that, although $\beta = 1$ to $2 \ \times 10^{21}$ s^{-1} reproduces the ER excitation functions of ^{19}F + ^{180}Hf and ^{19}F + ^{181}Ta systems over the entire range of excitation energy, higher values of $\beta = 2{-}3 \times 10^{21}$ s^{-1} are required for the ^{19}F + ^{182}W system. Similar observations are also made in Fig. 3 where measured and calculated $\sigma_{\rm ER}$ normalized by $\sigma_{\rm cap}$ (obtained from CC calculations) are plotted. The necessity of a higher value for β for the ^{19}F + ^{182}W reaction possibly arises from the facts that: (a) the excitation energy of the CN for this system is about 5 MeV less than those of the other two systems, and (b) the parameters deciding the energy dependence of CELD [Eq. (6)] are not optimized for the present systems but are taken from an earlier work [15]. The latter aspect requires further investigation in future studies. However, the above values of β are in agreement with the theoretical estimate of the presaddle dissipation strength based on the chaos-weighted wall formula [48]. It can also be noted from Fig. 3 that $\frac{\sigma_{\rm ER}}{\sigma_{\rm cap}}$ reduces gradually with increasing $\chi_{\rm CN}$. This is as expected since fission becomes a more dominant decay mode in the CN with larger fissility.

VI. Summary and conclusions. ER excitation functions have been measured for three reactions in a similar range of excitation energies in order to look for stabilizing effects of the $Z = 82$ shell closure against fission. The systems have been chosen in such a way that the three compound nuclei, formed in these reactions, have same number of neutrons ($N = 118$) but different numbers of protons ($Z = 81$, 82, 83). A not-so-heavy projectile ($A_p < 20$) has been chosen to ensure that the effect of NCNF on ER formation is not severe. The three targets also have quite similar structural features. Entrance channel parameters for the three reactions being comparable, the presence of NCNF, if any, is expected to affect ER formation in the three reactions quite similarly. Measured cross sections have been compared with SM predictions. The model includes shell effect in the level density, shell correction in the fission barrier, K orientation, and CELD. The reduced dissipation coefficient is the only adjustable parameter. It is found that the ER excitation functions can be reasonably reproduced with values of β in the range of 1–3 $\times 10^{21}$ s^{-1}. The ratio $\frac{\sigma_{ER}}{\sigma_{cap}}$ decreases with increasing fissility of the CN in the similar range of excitation energies. No significant and abrupt deviations have been found in the results obtained from ^{19}F + ^{181}Ta as evidence in favor of the stabilizing effects of the $Z = 82$ shell closure against fission. For further validation of this conclusion, a more exclusive measurement of individual exit channel cross sections in such reactions can be carried out in the future.

Acknowledgments. The authors thank the Pelletron staff of IUAC for excellent support throughout the experiment, Abhilash S. R. for assistance in fabricating isotopically enriched thin targets, and Dr. E. Prasad for providing the ^{180}Hf target.

[1] N. Bohr and J. A. Wheeler, Phys. Rev. **56**, 426 (1939).
[2] O. Hahn and F. Strassmann, Naturwissenschaften **27**, 11 (1939); L. Meitner and O. R. Frisch, Nature (London) **143**, 239 (1939); O. R. Frisch, *ibid.* **143**, 276 (1939).
[3] M. G. Mayer, Phys. Rev. **74**, 235 (1948); O. Haxel, J. H. D. Jensen, and H. E. Suess, *ibid.* **75**, 1766 (1949); M. G. Mayer, *ibid.* **75**, 1969 (1949); **78**, 16 (1950); **78**, 22 (1950).
[4] A. Sobiczewski, F. A. Gareev, and B. N. Kalinkin, Phys. Lett. **22**, 500 (1966).
[5] https://iupac.org/what-we-do/periodic-table-of-elements/.
[6] J. H. Hamilton, S. Hofmann, and Yu. Ts. Oganessian, Annu. Rev. Nucl. Part. Phys. **63**, 383 (2013).
[7] D. Vermeulen, H.-G. Clerc, C.-C. Sahm, K.-H. Schmidt, J. G. Keller, G. Münzenberg, and W. Reisdorf, Z. Phys. A **318**, 157 (1984).
[8] A. N. Andreyev, D. Ackermann, S. Antalic, I. G. Darby, S. Franchoo, F. P. Heßberger, S. Hofmann, M. Huyse, P. Kuusiniemi, B. Lommel, B. Kindler, R. Mann, G. Münzenberg, R. D. Page, Š. Šáro, B. Sulignano, B. Streicher, K. Van de Vel, P. Van Duppen, and D. R. Wiseman, Phys. Rev. C **72**, 014612 (2005).
[9] S. Nath, P. V. Madhusudhana Rao, S. Pal, J. Gehlot, E. Prasad, G. Mohanto, S. Kalkal, J. Sadhukhan, P. D. Shidling, K. S. Golda, A. Jhingan, N. Madhavan, S. Muralithar, and A. K. Sinha, Phys. Rev. C **81**, 064601 (2010).
[10] S. Nath, J. Gehlot, E. Prasad, J. Sadhukhan, P. D. Shidling, N. Madhavan, S. Muralithar, K. S. Golda, A. Jhingan, T. Varughese, P. V. Madhusudhana Rao, A. K. Sinha, and S. Pal, Nucl. Phys. **A850**, 22 (2011).
[11] G. Mohanto, N. Madhavan, S. Nath, J. Sadhukhan, J. Gehlot, I. Mazumdar, M. B. Naik, E. Prasad, I. Mukul, T. Varughese, A. Jhingan, R. K. Bhowmik, A. K. Sinha, D. A. Gothe, P. B. Chavan, S. Pal, V. S. Ramamurthy, and A. Roy, Nucl. Phys. A **890-891**, 62 (2012).
[12] G. Mohanto, N. Madhavan, S. Nath, J. Gehlot, I. Mukul, A. Jhingan, T. Varughese, A. Roy, R. K. Bhowmik, I. Mazumdar, D. A. Gothe, P. B. Chavan, J. Sadhukhan, S. Pal, M. Kaur, V. Singh, A. K. Sinha, and V. S. Ramamurthy, Phys. Rev. C **88**, 034606 (2013).
[13] R. du Rietz, E. Williams, D. J. Hinde, M. Dasgupta, M. Evers, C. J. Lin, D. H. Luong, C. Simenel, and A. Wakhle, Phys. Rev. C **88**, 054618 (2013).
[14] A. Shamlath, E. Prasad, N. Madhavan, P. V. Laveen, J. Gehlot, A. K. Nasirov, G. Giardina, G. Mandaglio, S. Nath, T. Banerjee, A. M. Vinodkumar, M. Shareef, A. Jhingan, T. Varughese, DVGRKS Kumar, P. Sandya Devi, Khushboo, P. Jisha, N. Kumar, M. M. Hosamani, and S. Kailas, Phys. Rev. C **95**, 034610 (2017).
[15] A. R. Junghans, M. de Jong, H.-G. Clerc, A. V. Ignatyuk, G. A. Kudyaev, and K.-H. Schmidt, Nucl. Phys. A **629**, 635 (1998).
[16] A. Chaudhuri, T. K. Ghosh, K. Banerjee, S. Bhattacharya, J. Sadhukhan, C. Bhattacharya, S. Kundu, J. K. Meena, G. Mukherjee, R. Pandey, T. K. Rana, P. Roy, T. Roy, V. Srivastava, and P. Bhattacharya, Phys. Rev. C **91**, 044620 (2015).
[17] K. Nishio, A. N. Andreyev, R. Chapman, X. Derkx, C. E. Düllmann, L. Ghys, F. P. Heßberger, K. Hirose, H. Ikezoe, J. Khuyagbaatar, B. Kindler, B. Lommel, H. Makii, I. Nishinaka, T. Ohtsuki, S. D. Pain, R. Sagaidak, I. Tsekhanovich, M. Venhart, Y. Wakabayashi, and S. Yan, Phys. Lett. B **748**, 89 (2015).
[18] T. Banerjee, S. R. Abhilash, D. Kabiraj, S. Ojha, G. R. Umapathy, M. Shareef, P. V. Laveen, H. Duggal, R. U. Amarnadh, J. Gehlot, S. Nath, and D. Mehta, Vacuum **144**, 190 (2017).
[19] A. K. Sinha, N. Madhavan, J. J. Das, P. Sugathan, D. O. Kataria, A. P. Patro, and G. K. Mehta, Nucl. Instrum. Methods Phys. Res., Sect. A **339**, 543 (1994).
[20] Khushboo, S. Mandal, S. Nath, N. Madhavan, J. Gehlot, A. Jhingan, N. Kumar, T. Banerjee, G. Kaur, K. Rojeeta Devi, A. Banerjee, Neelam, T. Varughese, D. Siwal, R. Garg, I. Mukul, M. Saxena, S. Verma, S. Kumar, B. R. Behera, and P. Verma, Phys. Rev. C **96**, 014614 (2017).
[21] S. Nath, Comput. Phys. Commun. **179**, 492 (2008); **180**, 2392 (2009).
[22] R. J. Charity, J. R. Leigh, J. J. M. Bokhorst, A. Chatterjee, G. S. Foote, D. J. Hinde, J. O. Newton, S. Ogaza, and D. Ward, Nucl. Phys. A **457**, 441 (1986).
[23] P. Fröbrich and I. I. Gontchar, Phys. Rep. **292**, 131 (1998).
[24] A. J. Sierk, Phys. Rev. C **33**, 2039 (1986).
[25] W. D. Myers and W. J. Swiatecki, Nucl. Phys. **81**, 1 (1966).
[26] J. P. Lestone and S. G. McCalla, Phys. Rev. C **79**, 044611 (2009).
[27] J. P. Lestone, Phys. Rev. C **59**, 1540 (1999).
[28] A. V. Ignatyuk, M. G. Itkis, V. N. Okolovich, G. M. Smirenkin, and A. Tishin, Yad. Fiz. **21**, 485 (1975) [Sov. J. Nucl. Phys. **21**, 255 (1975)].

[29] W. Reisdorf, Z. Phys. A **300**, 227 (1981).
[30] S. Bjørnholm, A. Bohr, and B. R. Mottelson, in *Proceedings of the International Conference on the Physics and Chemistry of Fission, Rochester, 1973* (IAEA, Vienna, 1974), Vol. 1, p. 367.
[31] A. V. Ignatyuk, G. N. Smirenkin, M. G. Itkis, S. I. Mul'gin, and V. N. Okolovich, Fiz. Elem. Chastits At. Yadra **16**, 709 (1985) [Sov. J. Part. Nucl. **16**, 307 (1985)].
[32] V. I. Zagrebaev, Y. Aritomo, M. G. Itkis, Yu. Ts. Oganessian, and M. Ohta, Phys. Rev. C **65**, 014607 (2001).
[33] M. Ohta, in *Proceedings on Fusion Dynamics at the Extremes, Dubna, 2000*, edited by Yu. Ts. Oganessian and V. I. Zagrebaev (World Scientific, Singapore, 2001), p. 110.
[34] H. A. Kramers, Phys. (Amsterdam) **7**, 284 (1940).
[35] P. Grangé, L. Jun-Qing, and H. A. Weidenmüller, Phys. Rev. C **27**, 2063 (1983).
[36] K. H. Bhatt, P. Grangé, and B. Hiller, Phys. Rev. C **33**, 954 (1986).
[37] T. Banerjee, S. Nath, and S. Pal, Phys. Lett B. **776**, 163 (2018).
[38] T. Banerjee, S. Nath, and S. Pal, Phys. Rev. C **99**, 024610 (2019).
[39] A. K. Nasirov, G. Mandaglio, M. Manganaro, A. I. Muminov, G. Fazio, and G. Giardina, Phys. Lett. B **686**, 72 (2010).
[40] K. Hagino, N. Rowley, and A. T. Kruppa, Comput. Phys. Commun. **123**, 143 (1999).
[41] T. Banerjee, S. Nath, A. Jhingan, N. Saneesh, M. Kumar, A. Yadav, G. Kaur, R. Dubey, M. Shareef, P. V. Laveen, A. Shamlath, Md. Moin Shaikh, S. Biswas, J. Gehlot, K. S. Golda, P. Sugathan, and S. Pal, Phys. Rev. C **96**, 014618 (2017).
[42] A. Shrivastava, S. Kailas, A. Chatterjee, A. M. Samant, A. Navin, P. Singh, and B. S. Tomar, Phys. Rev. Lett. **82**, 699 (1999).
[43] A. Chaudhuri, T. K. Ghosh, K. Banerjee, S. Bhattacharya, J. Sadhukhan, S. Kundu, C. Bhattacharya, J. K. Meena, G. Mukherjee, A. K. Saha, M. A. Asgar, A. Dey, S. Manna, R. Pandey, T. K. Rana, P. Roy, T. Roy, V. Srivastava, P. Bhattacharya, D. C. Biswas, B. N. Joshi, K. Mahata, A. Shrivastava, R. P. Vind, S. Pal, B. R. Behera, and V. Singh, Phys. Rev. C **92**, 041601(R) (2015).
[44] C. Simenel, D. J. Hinde, R. du Rietz, M. Dasgupta, M. Evers, C. J. Lin, D. H. Luong, and A. Wakhle, Phys. Lett. B **710**, 607 (2012).
[45] A. N. Andreyev, M. Huyse, P. Van Duppen, C. Qi, R. J. Liotta, S. Antalic, D. Ackermann, S. Franchoo, F. P. Heßberger, S. Hofmann, I. Kojouharov, B. Kindler, P. Kuusiniemi, S. R. Lesher, B. Lommel, R. Mann, K. Nishio, R. D. Page, B. Streicher, Š. Šáro, B. Sulignano, D. Wiseman, and R. A. Wyss, Phys. Rev. Lett. **110**, 242502 (2013).
[46] P. D. Shidling, N. Madhavan, V. S. Ramamurthy, S. Nath, N. M. Badiger, S. Pal, A. K. Sinha, A. Jhingan, S. Muralithar, P. Sugathan, S. Kailas, B. R. Behera, R. Singh, K. M. Varier, and M. C. Radhakrishna, Phys. Lett. B **670**, 99 (2008).
[47] A. Chaudhuri, A. Sen, T. K. Ghosh, K. Banerjee, J. Sadhukhan, S. Bhattacharya, P. Roy, T. Roy, C. Bhattacharya, M. A. Asgar, A. Dey, S. Kundu, S. Manna, J. K. Meena, G. Mukherjee, R. Pandey, T. K. Rana, V. Srivastava, R. Dubey, G. Kaur, N. Saneesh, P. Sugathan, and P. Bhattacharya, Phys. Rev. C **94**, 024617 (2016).
[48] G. Chaudhury and S. Pal, Phys. Rev. C **65**, 054612 (2002).